

Design and Simulation of Internal Planetary Wheel Plunger-Type Ring Molding Machine for Biomass Pellets

Xuehong De,^{a,#} Bowen Zhang,^{a,#} Jingyan Zhao,^b Wenbin Guo,^{a,*} Jianchao Zhang,^a Jianwen Kang,^a and Haoming Li^a

Key components of the existing external meshing dorsal spine plunger-type molding machine were modeled in three dimensions, and the fatigue life analysis of the molding machine spindle was carried out by using Ansys software. Due to the nonlinear mechanical behavior of the material ring mold, and pressure roller in the granulation process, there are a lot of contacts and collisions. Using the linear mechanics model is difficult to analyze. To achieve more accurate and realistic results, an Edem-Ansys joint coupled simulation was carried out for the pressure roller and ring mold engagement process. The results showed that the stress concentration point and fatigue weak region of the spindle occurred at the shaft cross-section, where the stress value should be less than 0.75 F . The maximum stresses and strains in the engagement process of the pressure roller and the ring die body occurred at the engagement point. The maximum values of deformation, stress, and strain were 0.039 mm, 412 MPa, and 0.002 mm/mm, respectively, which are all within the reasonable range and meet the design requirements.

DOI: 10.15376/biores.19.3.5599-5609

Keywords: Ring molding machine; Structural design; Fatigue life; Coupled simulation

Contact information: a: College of Mechanical and Electrical Engineering, Inner Mongolia Agricultural University, Hohhot, PR China; b: College of Fine Art and Design, Heihe University, Heihe, PR China; #: These authors contributed equally to this work; *Corresponding author: wenbingwb2000@sina.com

INTRODUCTION

Biomass curing and molding technology can be used to process agricultural and forestry residues into blocks, rods, or pellets with certain shapes and densities through mechanical compression methods. These pellets have high calorific value, are non-polluting, are convenient for storage and transportation, and have become a hot spot of biomass curing and molding research both at home and abroad. According to domestic and international research, the main technical problems of ring molding include: a low effective compression molding rate of some of the ring molding machines put into production; and the traditional ring molding machine adopts the extrusion form of the outer curved surface of the die rolls, which is characterized by high cost, high energy consumption, and serious wear and tear of the key components (Huo *et al.* 2010; Yi 2011; Mahalingam *et al.* 2020).

Based on the above problems, in this work an internally meshing planetary wheel plunger-type biomass ring molding machine was designed. The press rolls of the molding machine are surrounded by several rows of compression cams at an angle of 45° to their axes. By this arrangement, in the process of rotation to achieve the compression of the convex die and the ring mold molding the holes will be in the correct position of engagement. While completing the efficient compression of materials, the described

system can effectively reduce the squeezing force and friction between the pressure roller and the ring die, thus solving the problem of serious wear and tear of key components and high energy consumption of the same type of molding machine. (De *et al.* 2020).

Lifetime Theory

The material S-N curve characterizes the relationship between the stresses applied to the material and the fatigue life were considered in earlier work (Dinh and Vu 2022). The fatigue life N represents the number of stress or strain cycles experienced by the specimen before fatigue damage at the stress ratio R , as shown in Fig. 1.

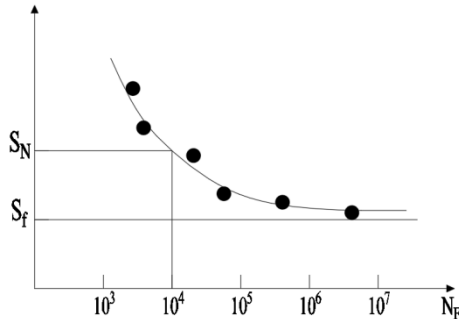


Fig. 1. S-N curve of the material

Figure 1 shows that the smaller the stress S to which the specimen is subjected, the longer its fatigue life is under a certain stress ratio. When S_f is less than the fatigue limit, the specimen will not be damaged. The steel takes the 10^7 stress level corresponding to the secondary stress cycle as the fatigue limit of the steel. The S_N value is the fatigue strength corresponding to the material life of N . The S-N curve is expressed as follows,

$$N = CS^{-m} \quad (1)$$

where m and C are constants related to the strength of the material. Taking logarithms on both sides of the above equation, the following equation is obtained.

$$\lg N = \lg C - m \lg S \quad (2)$$

Thus, the above equation can also then be written as the following equation for the p -S-N curve of the material,

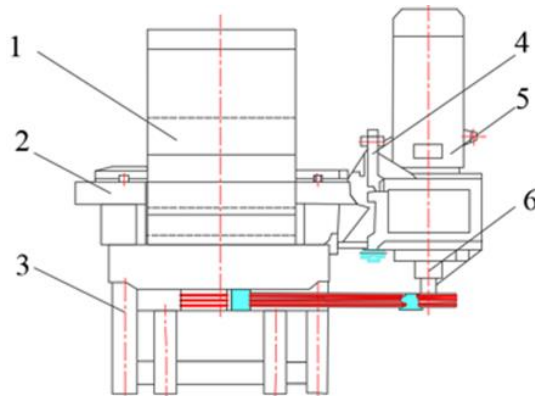
$$\lg N_p = a_p - b_p \lg S \quad (3)$$

where N_p is the fatigue life at a survival probability of p , and a_p , b_p are constants for the material.

Overall Structural Design of Molding Machine

Structural design of molding machine

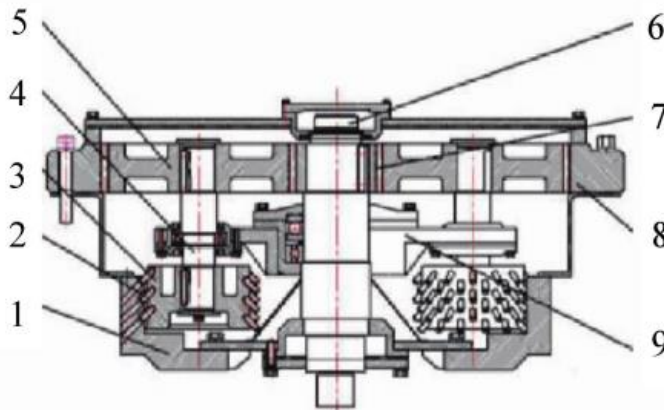
As shown in Fig. 2, the internal meshing planetary wheel plunger-type biomass ring molding machine mainly consists of the host bracket, host device, feeding funnel, power bracket, power source, belt wheel, *etc.*



1. Feeding funnel; 2. Host device; 3. Host bracket; 4. Power bracket; 5. Power source; 6. Belt wheel

Fig. 2. Overall structure of the molding machine

As shown in Fig. 3, the host device is the core of the design for the rotary body structure, including the spindle, ring mold body, compression cam, pressure roller body, pressure roller shaft, coupling seat, straight-toothed cylindrical internal gear, pressure roller shaft gear, spindle gear, and so on.



1. Ring mold body; 2. Compression cam; 3. Pressure roller body; 4. Pressure roller shaft; 5. Pressure roller shaft gear; 6. Spindle; 7. Spindle gear; 8. Straight-toothed cylindrical internal gear; 9. Coupling seat

Fig. 3. Host device

When working, the power output will be provided through the reducer with the narrow V-belt transmission to the spindle, driven by the spindle gear and two pressure roller gear within the meshing straight tooth cylindrical gear rotation, constituting a planetary wheel structure. The main shaft gear is a sun wheel, while the pressure roller shaft gear is a planetary wheel, and the internal meshing cylindrical gear is bolted to the bracket. Two pressure roller shaft gears are arranged symmetrically on both sides of the main shaft, driving the pressure roller shaft and the pressure roller body to rotate around the main shaft in the ring mold body. The rollers are equipped with a series of 45° plungers, which engage the mold holes, which are evenly distributed in the ring mold body in the correct position.

At this time, the material is fed into the rolling area through the feeding funnel and enters between the ring mold body and the pressure roller body. Under the action of friction between the material and the ring mold body and the material and the pressure roller body, part of the material is pressed into the molding hole. At the same time, the compression cam acts on the pressure roller body gradually and the corresponding ring mold forms a hole for position engagement and is pressed into the molding hole. The material continues to be pressed into the molding hole, after which the convex mold is gradually separated. During each rotation of the pressure roller body, the ring die molding hole in the material has to go through the filling and extrusion process. The initially loose biomass material gradually enters into the molding hole in a process of layer-by-layer extrusion molding, and finally it reaches a certain density and length of the particles of fuel, whereupon it is extruded out of the molding hole.

Design of molding machine drive scheme

The rotation between the pressure roller and the ring die must be synchronized to ensure that the speed of the pressure roller and the ring die are equal during the engagement process and that there is no interference or collision between the two. During the design of the transmission system, the ring mold and the pressure roller must rotate at the same speed. The design scheme is to act directly on the spindle of the ring mold machine, and then act on the pressure roller through the gear transmission. The transmission chain of this transmission method is shorter, the energy dissipation is less, and the overall size of the design is moderate. As shown in Fig. 4, the motor and reducer transfer the power to the spindle *via* the narrow V-belt, which drives the spindle to rotate, and the spindle and the double-pressure roller shaft rotate through the gear pair, which further constitutes the planetary wheel mechanism through the internal meshing of the ring mold body gear pair.

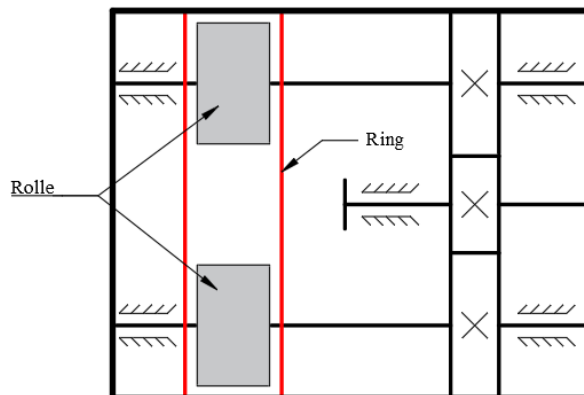
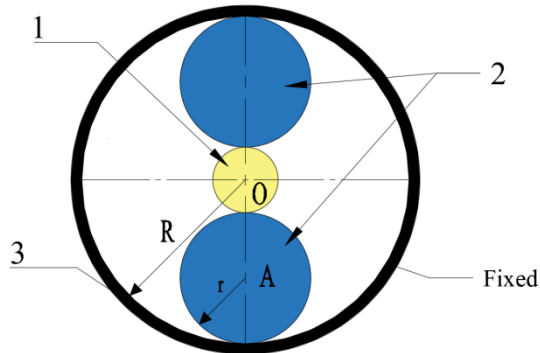


Fig. 4. Transmission scheme

Ring Molding Machine Parameters

When the friction coefficient of the material is determined, a larger mold roll ratio results in lower productivity (Li *et al.* 2015). The minimum value of the mold roll ratio should be in line with the formula $\mu \geq (1 + \sin \theta)$. The angle θ is equal to the larger value of the friction angle between the material and the pressure roller, between the material and the ring die body. This preliminary design is for a compression molding test on corn stover and wood chips. The friction coefficient between corn stover and metal is 0.42 to 0.51, and

the friction coefficient between wood chips and metal is 0.2 to 0.6. After comprehensive consideration, the mold roll ratio was selected as 2.5 (Suo 2022).



1. Spindle gear; 2. Pressure roller gear; 3. Ring mold internal gear

Fig. 5. Transmission dimension relationship in the molding area

Figure 5 shows the ring die particle molding machine gear size relationship. The procedure involves setting the ring mold spindle gear 1 tooth number for Z_1 , pressure roller gear 2 tooth number for Z_2 , gear module for m , pressure roller and ring mold transmission ratio as i , the ring mold inner radius and pressure roller meshing circle as R and r , respectively. These last two variables are set so as to meet the following relationship:

$$R = \mu r, OA = R - r = \frac{m}{2} Z_1 + \frac{m}{2} Z_2 \quad (4)$$

Table 1. The Parameters of Molding Machine

Parameter	Value
Motor Power (kw)	15
Plunger Number	72
Number of Molding Hole	228
Diameter of Compression Cam (mm)	8
Diameter of Molding Hole(mm)	8
Diameter of Compression Roller Cam (mm)	160
Ring Die Hole Diameter (mm)	540
Diameter of Straight-Toothed Cylindrical Internal Gear (mm)	160
Number of Teeth of Roll Shaft Gear	65
Gear Module	3
Overall Dimension (L×W×H)/(m×m×m)	1.12×1.0×1.07
Machine Mass (kg)	1450

Design of Ring Mold

Die hole structure and parameters

The ring mold dies hole determines the combustion performance of biomass-forming pellets, the output of forming pellets, and the ring die life. The structural parameters of the mold holes include the effective length of the mold holes, mold hole length-to-diameter ratio, mold hole shape, mold hole roughness, arrangement of the mold hole, and opening rate.

The effective length of the mold hole is the length of the mold hole in the molding process. A longer mold hole will result in a longer residence time of the material, and better quality molded particles are obtained. According to the value often taken by the existing equipment, the effective length of the mold hole is 40 mm. The mold-hole L/D ratio is the ratio of the effective length of the mold hole and the diameter of the hole. The mold-hole L/D ratio has an impact on the molding effect of the particles, such as density, hardness, and other indicators. The empirical range of the L/D ratio is 5 to 13. According to the value often taken by the existing equipment, this L/D ratio was designed as 5.

The ring mold holes have more shapes, generally dominated by circular cross-sections, and this design is circular cross-section. The roughness of the inner surface of the mold hole is positively correlated with the resistance of the particles in the hole. By the national standards, the roughness of the mold hole in this case was set to 1.6 (He *et al.* 2020). The die holes on the ring mold are usually neatly arranged and staggered in two ways. The neatly arranged way is susceptible to the cracking of the ring mold body, in which the stress state is poor, and the opening rate is low. Staggered ring molds have better stress characteristics, are less prone to cracking, and have a higher mold opening rate. The hole rate on the ring mold has a great role in improving the production efficiency, under the premise of guaranteeing the strength of the ring mold, it should be densely distributed as much as possible, so this arrangement was designed as a staggered arrangement (Li 2000).

Selection of Ring Mold and Pressure Roller Material

Considering the working intensity of the ring mold, the ring mold materials used are carbon structural steel, alloy steel, and stainless steel. Alloy structural steel, such as 40Cr, 35CrMo, *etc.*, with heat treatment hardness of more than 50HRC, has relatively good comprehensive mechanical properties. The 40Cr alloy structural steel was selected as the ring mold material because its strength and wear resistance are relatively good, and the cost is relatively low. To enhance the surface strength, the surface is subjected to the real air quenching heat treatment process. As the material between the mold roll cannot be the same, the pressure roller material is selected after carburization treatment of 20CrMnTi. The hardness after carburization is HRC52 to 54 (Wu *et al.* 2003).

Molding Machine Modeling

Figure 6 shows a 3D model and a photograph of the molding machine.

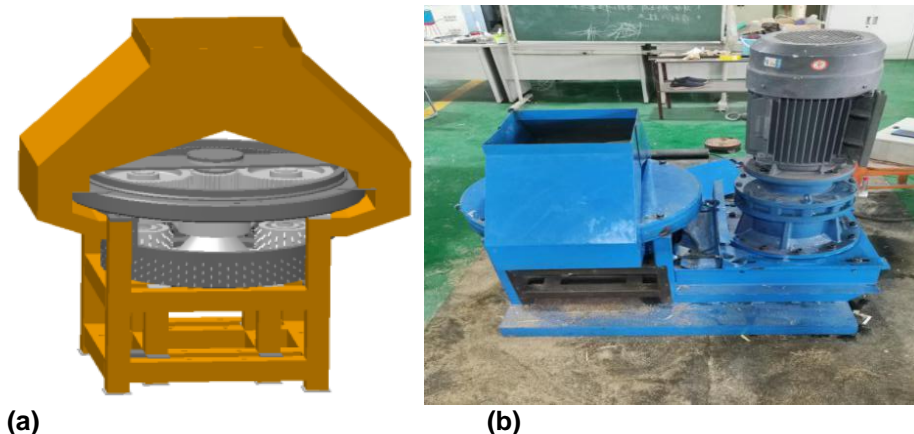


Fig. 6. Ring molding machine diagram

SIMULATION

Spindle Life Analysis

The spindle was statically analyzed by use of Ansys software, and the fatigue analysis parameters were set to obtain the fatigue-breaking zone of the spindle. Under the action of alternating load and torque coupling, the local enlargement of the spindle damage zone of the molding machine is shown in Fig. 7.

Figure 7 shows that the main damage area of the spindle is at the variable section of the bearing end of the shaft, close to the gear shaft end, with a damage value of 3367.1. Its location is a common location for shaft stress concentration (Jin 2017). This result indicates that when the shaft reaches the end of its service life, cracks will first develop at this location and begin to spread to the surrounding area.

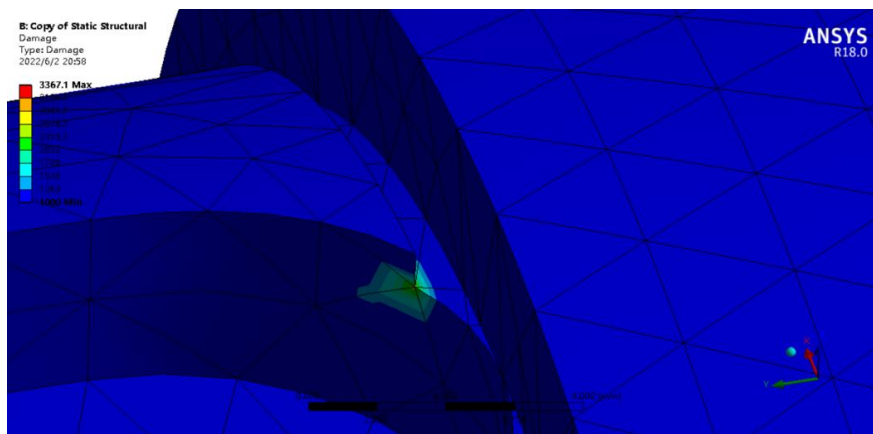


Fig. 7. Localized enlarged view of fatigue damage area

In order to extend the life of the spindle, it is important to know the stress requirements of the shaft, so it is important to simulate the life of the shaft. The life simulation of the spindle is carried out, and the fatigue distribution map of the spindle, as well as the fatigue sensitivity curve, which are shown in Figs. 8 and 9.

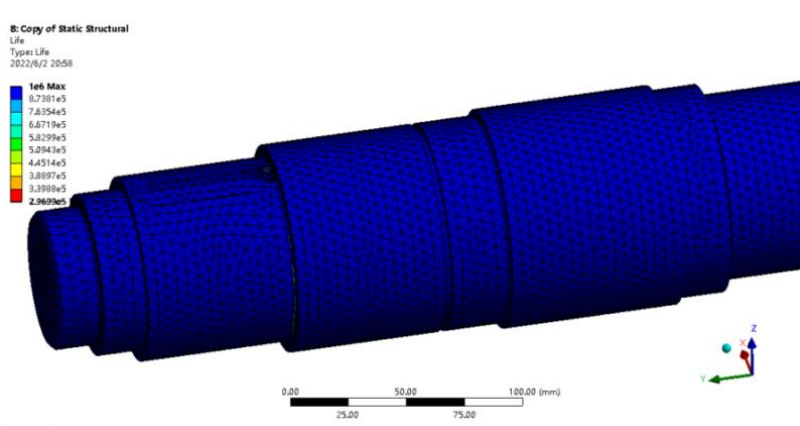


Fig. 8. Spindle fatigue distribution area

As shown in Fig. 8, the fatigue life of the main shaft meets the requirements in most of the regions. At the bearing end near the variable section of the gear shaft, the life value

starts to decrease, and the minimum life is 2.96×10^3 , which is the same as the maximum stress as well as the location where the maximum damage zone occurs.

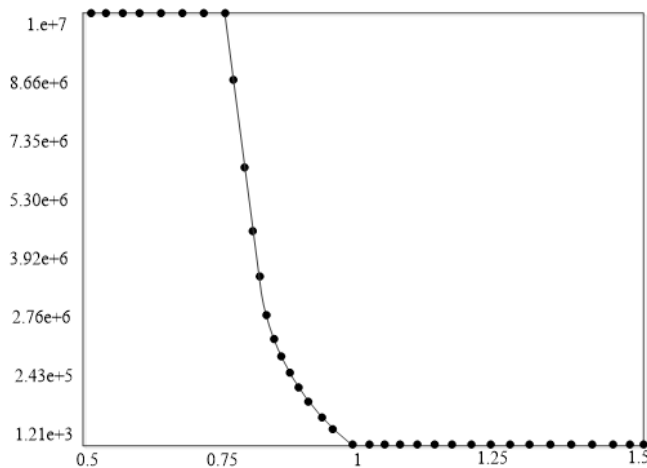


Fig. 9. Fatigue sensitivity curve

When the stress applied to the spindle is below $0.75F$, the increase in load hardly affects the fatigue life. When the stress applied to the spindle, F , is increased from 0.75 to 1.0, the fatigue life of the spindle changes significantly, and its life decreases from 1×10^7 to 1.21×10^3 . Therefore, the stress on the spindle should be guaranteed to be less than $0.75F$.

Coupled Simulation of Pressure Roll and Ring Die Engagement Processes by Edem-Ansys Combination

Caragana are the raw material for this simulation, and the shape of the particle simulation is shown in Fig. 10(a). For the phenomenon of fracture and deformation during the extrusion of caragana, the intra-particle contact models were selected as Hertz-Mindlin with the *Hertz-Mindlin with bonding built-in Compatibility* model and the *Hertz-Mindlin with JKR* model. The contact model between the particles and the machine model was the *Hertz-Mindlin with Archard Wear built-in Compatibility* wear contact model, which was used to simulate the wear of the device. After setting the parameters, the pellet plant is created and the ring die body is fed to simulate the pellet molding process, as shown in Fig. 10(b).

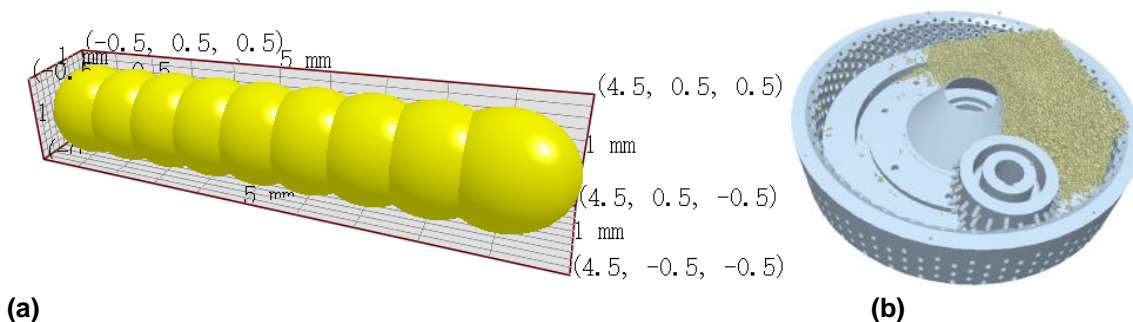


Fig. 10. Edem simulation

Because the simulation results of Edem are limited to the global force, the mechanical results are relatively single. Ansys cannot provide a discrete material mechanical analysis program, so Ansys and Edem were used in a coupled simulation. Combining Edem's discrete element force application algorithm and Ansys's multivariate mechanical analysis program creates a model of the real force situation. The model data of Edem is directly imported into Ansys. After the data correlation, the mesh division adopts the default tetrahedral mesh division, and most of the area is divided into 8 mm mesh; for the area in contact with the pressure roller and the ring die body, the mesh is divided into 1 mm. After the mesh division, the ring die body is subjected to displacement, stress, and strain analysis, and the results are shown in Fig. 11.

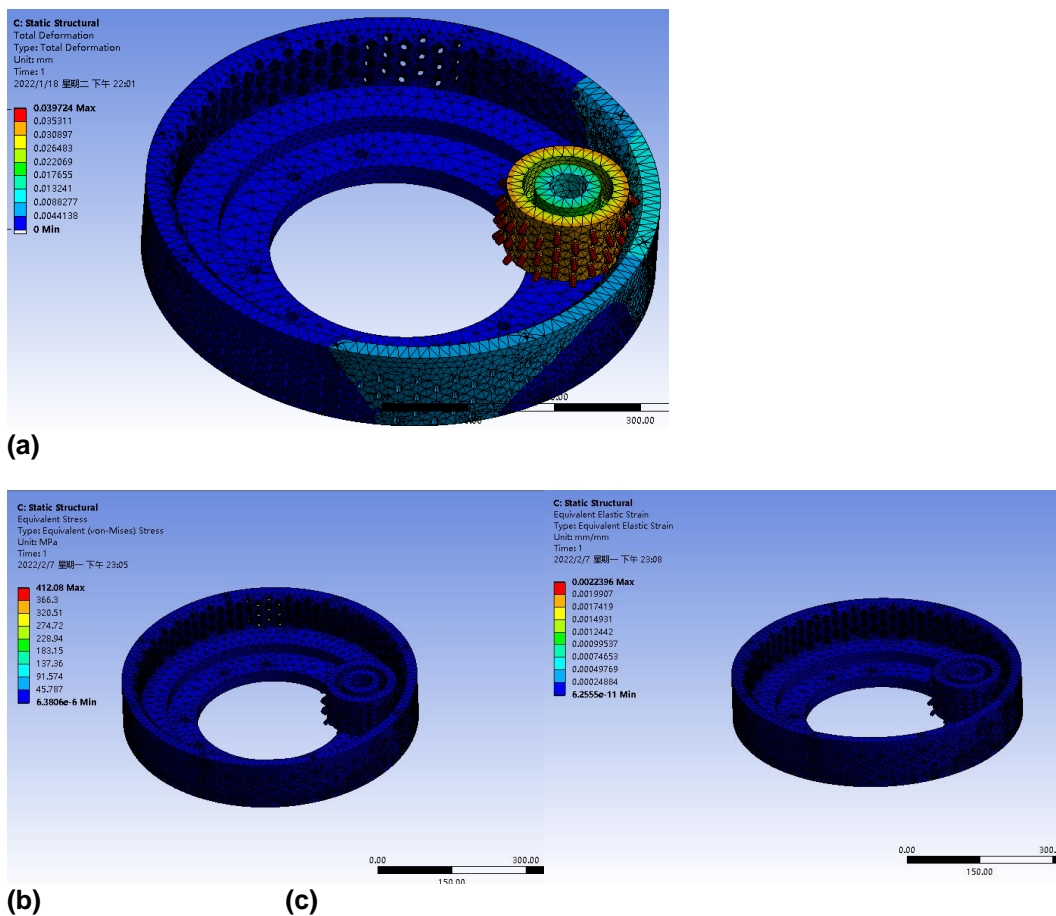


Fig. 11. Edem-Ansys coupled simulation results

The maximum value of displacement change of the pressure roller is at the front end of the pressure roller plunger. The maximum displacement deformation area of the ring mold body is in the upper edge of the contact area of the ring mold pressure roller. The maximum point of displacement deformation occurs at the front end of the pressure roller, and the deformation value is 0.039 mm. The maximum point of stress occurs at the contact point of the pressure roller body and the ring die body, and the maximum stress value is 412 MPa, which is less than the permissible stress value of the material 691 MPa. The strain analysis shows that the maximum value of strain is 0.002 mm/mm, which satisfies the requirement. In both the deformation and stress analysis results, the maximum strain occurrence and the stress maximum point are the same. The results are within a reasonable

range, which indicates that the ring die body and the pressure roller structure can meet the requirements of the design working conditions. For the problem of serious wear of the molding machine, its wear mainly occurs in the contact area between the plunger and the mold hole, and structural improvement through these two parts is something that can be studied in the future.

CONCLUSIONS

1. An internally meshing planetary wheel plunger-type biomass ring molding machine was designed to reduce the friction and wear in the molding process compared with the traditional molding machine. The wear of the molding machine occurs mainly in the contact area between the plunger and the mold hole, and structural improvement through these two parts is something that can be investigated in the future. The molding machine parts were modeled, and the three-dimensional model was drawn to prepare for future simulation.
2. The stress concentration point and fatigue weak region of the spindle is predicted to occur in the region of the shaft cross-section shape mutation. Fatigue life analysis of the spindle shows that the spindle force should guarantee to be less than $0.75F$, so the spindle can have a long service life.
3. EDEM-Ansys coupled simulation of the molding process demonstrated that the maximum deformation in the pressure roller and ring mold body engagement process occurs in the front of the pressure roller plunger, with a displacement deformation of 0.039 mm and strain maximum value of 0.002 mm/mm. The maximum stress is concentrated in the point of engagement. The maximum stress value of 412 MPa is less than the permissible stress value of the material 691 MPa, which meets the design requirements.

ACKNOWLEDGMENTS

The authors are grateful to Bowen Zhang from Inner Mongolia Agricultural University, Hohhot, China, for help with laboratory analysis work. The authors are also grateful for the financial support of the National Natural Science Foundation of China (NSFC) project (51766016; 31960365; 32060414).

REFERENCES CITED

- De, X. H., Wu, G. F., Li, N. D., Zhang, J. C., Guo, W. B., and Li, Z. (2020). "Design and testing of an internal mesh planetary wheel plunger-type biomass ring molding machine," *Journal of Agricultural Machinery* 51(10), 379-386. DOI: 10.6041/j.issn.1000-1298.2020.10.043
- Dinh, Q. C., and Vu, D. C. (2022). "Estimation of overall fatigue life of jack-up leg structure," *Civil Engineering Journal* 8(3), 488-504. DOI: 10.28991/CEJ-2022-08-03-06

- Huo, L. L., Hou, S. L., Tian, Y. S., Zhao, L. X., Meng, H. B., and Sun, H. (2010). “Analysis of wear loss of biomass solid fuel molding machine pressure rollers,” *Journal of Agricultural Engineering* 26(07), 102-106. DOI: 10.3969/j.issn.1002-6819.2010.07.018
- He, Y. B., Yan, Y. L., and Huang, J. (2020). “Analysis of different hole shapes in biomass curing and forming machine,” *Forest Industry* 57(02), 46-49. DOI: 10.19531/j.issn1001-5299.202002010
- Jin, S. (2017). *Improved Design and Experiment of Key Parts of External Meshing Plunger Type Pellet Molding Machine*, Beijing Forestry University, Beijing, China. DOI: 10.26949/d.cnki.gblyu.2017.000301
- Li, Z., Yu, G. S., Chen, Z. J., Yuan, X. Y., and Cao, L. Y. (2015). “Design and test of toothed-roller ring mold biomass forming machine,” *Journal of Agricultural Machinery* 46(05), 220-225. DOI: 10.6041/j.issn.1000-1298.2015.05.031
- Mahalingam, A., Nagappan, B., Jayaram, P., and Nagalingeswara, R. B. (2020) “Investigating the physio-chemical properties of densified biomass pellet fuels from fruit and vegetable market waste,” *Arabian Journal for Science and Engineering* 45(1), 563-574. DOI: 10.1007/s13369-019-04294-8
- Suo, B. (2022). *Design and Experimental Study of Internal Meshing Plunger Type Biomass Ring Molding Machine*, Inner Mongolia Agricultural University, Hohhot, China. DOI: 10.27229/d.cnki.gnmnu.2022.001007
- Wu, B. L., Yang, S. J., and Yao, J. H. (2003). “Theoretical analysis of meshing shock in gear transmission,” *Mechanical Science and Technology* 22(1), 55-57. DOI: 10.3321/j.issn:1003-8728.2003.01.018
- Yi, Y. T. (2011). *Research on Biomass Molding Influencing Factors and Design of Roll Forming Machine*, Northeastern University, Shenyang, China. DOI: 10.7666/d.J0104848

Article submitted: August 12, 2023; Peer review completed: September 16, 2023;
Revised version received: March 2, 2024; Accepted: March 3, 2024; Published: July 1, 2024.

DOI: 10.15376/biores.19.3.5599-5609